ADVANCED FUNCTIONAL MATERIALS
www.afm-journal.de

Luminescence of Nanodiamond Driven by Atomic Functionalization: Towards Novel Detection Principles

Vladimíra Petráková, Andrew Taylor, Irena Kratochvílová, František Fendrych, Jiří Vacík, Jan Kučka, Jan Štursa, Petr Cígler, Miroslav Ledvina, Anna Fišerová, Peter Kneppo, and Miloš Nesládek**

High biocompatibility, variable size ranging from ≈5 nm, stable luminescence from its color centers, and simple carbon chemistry for biomolecule grafting make nanodiamond (ND) particles an attractive alternative to molecular dyes for drug-delivery. A novel method is presented that can be used for remote monitoring of chemical processes in biological environments based on color changes from photoluminescent (PL) nitrogen-vacancy (NV) centers in ND. The NV luminescence is driven chemically by alternating the surface chemical potential by interacting atoms and molecules with the diamond surface. Due to the small ND size, the changes of the surface chemical potential modify the electric field profile at the diamond surfaces (i.e., band bending) and intermingle with the electronic NV states. This leads to changes in NV^-/NV° PL ratio and allows construction of optical chemo-biosensors operating in cells, with PL visible in classical confocal microscopes. This phenomenon is demonstrated on single crystal diamond containing engineered NV centers and on oxidized and hydrogenated ND in liquid physiological buffers for variously sized ND particles. Hydrogenation of NDs leads to quenching of luminescence related to negatively charged (NV^-) centers and as a result produces color shifts from NV^- (638 nm) to neutral NV° (575 nm) luminescence. How the reduction of diamond size increases the magnitude of the NV color shift phenomena is modeled.

1. Introduction

Nanodiamond (ND) particles with a size range of 5 to 100 nm can serve as a new type of optical marker for cellular imaging.[1–4] Strong ND photoluminescence (PL) originates from single photon producing nitrogen-vacancy (NV) color centers consisting of a substitutional nitrogen atom next to a vacancy that is engineered artificially in the diamond lattice. The nanoscale effects related to artificially engineered NV color centers attracted important attention to diamond due to applications ranging from quantum computing to cell imaging.[2–4] The luminescence from NV centers is extremely stable without any photobleaching or photoblinking[5–7] and compared to better known quantum dots, ND brings additional advantages such as high biocompatibility[8,9] and simple C-surface chemistry.[10,11] This allows grafting of biomolecules that are interesting for cellular targeting[12,13] or biomolecular drug delivery.[14–16] However, for very small ND particles (5 nm) blinking of NV centers was observed,[17] showing that the surface effects are of importance for stabilization of NV luminescence properties.

Here we describe how the surface chemistry effects can make the ND bulk luminescence sensitive to chemical processes ongoing at the ND surface, with the aim of using ND for monitoring a chemical environment such as surface charges or pH, cellular DNA/RNA hybridization, interaction with cell receptors, etc. The proposed method is based on the control of an electronic chemical potential at the

V. Petráková, Prof. P. Kneppo
Czech Technical University in Prague
Faculty of Biomedical Engineering
Sítná sq. 3105, 272 01 Kladno
Czech Republic
E-mail: vladimira.petrakova@fbmi.cvut.cz
A. Taylor, Dr. I. Kratochvílová, Dr. F. Fendrych
Institute of Physics
Academy of Sciences of the Czech Republic
v.v.i, Prague 8, Czech Republic
Dr. J. Vacík, J. Kučka, Dr. J. Štursa
Nuclear Physics Institute
Academy of Sciences of the Czech Republic
v.v.i, 250 68 Rez near Prague, Czech Republic
Dr. P. Cígler, Dr. M. Ledvina
Institute of Organic Chemistry and Biochemistry
Academy of Sciences of the Czech Republic
v.v.i., Flemingovo n. 2, 166 10 Prague 6, Czech Republic
Dr. A. Fišerová
Institute of Microbiology
Academy of Sciences of the Czech Republic
v.v.i., 142 20 Prague 4, Czech Republic
Prof. M. Nesládek
IMOMEC division, IMEC
Institute for Materials Research
University Hasselt
Wetenschapspark 1, B-3590 Diepenbeek, Belgium
E-mail: milos.nesladek@uhasselt.be

DOI: 10.1002/adfm.201101936

ND surfaces, which influences the surface band bending and is known to occur at variously terminated diamond surfaces.[18–20] It in this way changes the occupation of the luminescent NV centers that exist in neutral (NV°) or negative charge states (NV^-)[21,22] with different PL–zero phonon line (ZPL) emission wavelength properties. Therefore it is possible to control emission wavelength, i.e., 575 nm for NV° (ZPL) and 638 nm for NV^- (ZPL). The method explained below yields advantages over recently demonstrated ND Foerster resonance energy transfer (FRET),[23] where the FRET donor dye was replaced by a ND particle. FRET sensitivity scales as $1/r^6$ (where r is the interaction radius between the molecular event and the detection center, in case of FRET it is the distance bewteen the ND and the biomolecule), allowing induced luminescence shifts originating at the energy transfer between the ND donor and the acceptor dye for sizes of ≈5 nm. In our case, due to $1/r^2$ Columbic interactions, which result from the solution of the Poisson equation (see below) in combination with solution of the Schrödinger equation for deep lying NV defects,[24] we can observe chemically driven luminescence shifts up to larger distances, ≈20 nm in depth, which is calculated by modeling. This allows construction of optical ND chemo-biosensors with sizes of about 40 nm that are easily visible in classical confocal microscopes. This can be especially interesting for drug-delivery research and for monitoring chemical interactions occurring in cells based on covalent or non-covalent interactions with charged molecules such as DNA and with various surface terminations.

We demonstrate this mechanism on ND with hydrogenated and oxidized surfaces, which exhibit important differences in the surface chemical potential. We validate the model and ND size effect by comparing the results with a defect-free, chemical vapor deposition (CVD) grown IIa single crystal diamond (SCD) with electronic-grade surface polish (<0.1 nm), which was implanted to the nanometer depth with nitrogen and subsequently annealed to convert N to NV centers by the trapping of vacancies. Electric field penetration related and corresponding size effects of ND particles on luminescence is modeled mathematically. We show clearly why the size effect of nanoparticles is important with comparison to bulk single crystal CVD diamond (SCD),[25,26] as this allows a significant increase in the color shift magnitude.

2. Results and Discussion

2.1. Quenching of NV Luminescence on ND Particles

H-terminated diamond surfaces possess a high electric dipole moment that attracts negative polar ions, such as water adsorbates,[18,27] leading to creation of a hole accumulation layer at the surface for undoped diamond of a high purity with consequent upwards surface band bending, causing a generation of a 2D hole gas (2DHG) at the diamond surface and pinning of the Fermi level at the valence band maximum (E_{VBM}).[20,28] This effect is called surface transfer doping[19] and is used in many 2DHG diamond devices such as solution gate field-effect transistors (FETs).[29,30] We employ a very similar effect, i.e., changes of the chemical potential of variously terminated surfaces, but add into the system NV centers that are present in the band bending zone, to induce changes in the occupation of NV° and NV^- centers lying in the diamond subsurface. This effect has been clearly documented for single crystal, polycrystalline, and nanocrystalline diamond.[31,32] To determine exact band bending profiles, in our case one must calculate additionally with N and NV centers present in the diamond, both of which act as donors and therefore influence the band-bending zone. Based on the solution of the Schrödinger equation using density functional theory (DFT), NV° and NV^- centers have different ground state energy levels 1.2 eV and 2.0 eV (calculated by Goss et al.[24,33]). The Fermi level (E_F) energy will be reduced to be below the level of NV^- (NV°), therefore this state becomes unoccupied and cannot contribute to the luminescence (electron cannot be excited from this state). By controlling the band banding at the diamond surface one thus controls NV charge states to a certain depth and consequently the PL spectra. Color shifts in diamond affected by surface termination reported by our group[34] were also recently observed by another group[35] but their origin, which we model, was not explained. In general, hydrogen termination on undoped diamond surfaces leads to upwards band bending, i.e., the hole accumulation layer, while oxygen termination (with an electric dipole moment in the opposite direction) causes an opposite effect, i.e., the downwards band bending. If the particles are sufficiently small, i.e., in ≈10 nm scale, the surface transfer doping[19,20] could influence the NV luminescence in the whole particle, leading to optically detected luminescence shifts via relative shift of NV°/NV^- levels with respect to the E_F (i.e., the state occupation). The situation is illustrated in **Figure 1**.

2.2. Photoluminescence in ND

Particles of 20 to 50 nm size, produced from high-pressure high-temperature (HPHT) synthetic Ib diamond are very suitable for biologic applications due to the possibility of production of a high amount of stable NV centers. These provide sufficient luminescence contrast that is comparable to other biomarkers and retains advantages related to their nanodimension. To investigate the effect of PL shifts, HPHT ND particles containing approximately 200 ppm of N and with a peak size distribution at ≈40 nm and 100 nm were irradiated by protons using energy of 5.4 MeV to produce vacancies and subsequently annealed at 700 °C (see Experimental Section) to produce NV centers. Raman spectra taken in each step of the process confirmed the high quality of ND, similar to single crystal diamond, showing no visible non-diamond sp^2 structures (Figure S2, Supporting Information) that could negatively influence the surface charge interactions, i.e., reduce the sensitivity of the surface termination to the surface chemical potential as is the case for detonation ND.[36] **Figure 2**a shows the experimental data obtained for 40 nm ND for three different situations: oxidized surface, hydrogenated surface, and diamond after subsequent oxidation performed by annealing at 400 °C in air. According to our model, explained in detail in the Supporting Information, the NV^- luminescence with a ZPL at 638 nm is fully quenched after hydrogen termination, while the NV° luminescence is still visible. The NV^- luminescence can be restored again by

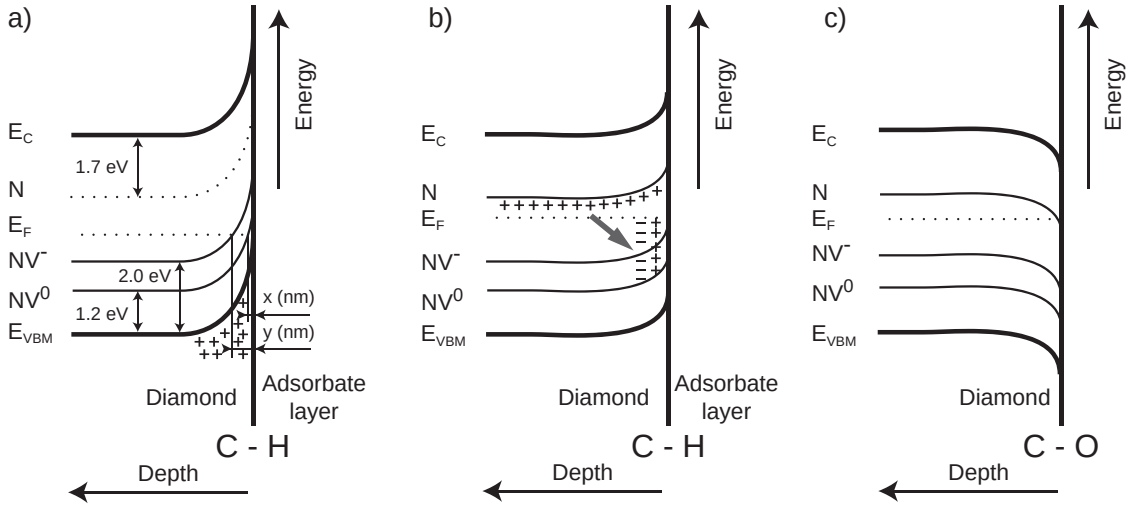

Figure 1. Schematic model of surface band bending for hydrogen terminated diamond containing NV centers with a) low content of nitrogen and b) high content of nitrogen. Nitrogen in the diamond lattice acts as an electron donor and electrons will compensate the holes accumulated at the surface, effectively reducing the surface band bending and inhibiting the influence of hydrogen termination on photoluminescence. Additional nitrogen influences the position of the Fermi level E_F in the band gap. c) Oxidized diamond surface with downward band bending, NV° and NV^- are occupied. *x* (nm) and *y* (nm) are regions of which the Fermi level crosses the NV^- and NV° energy, i.e., regions where the ground levels of NV^- and NV° are not occupied and therefore luminescence cannot occur.

annealing in air, leading to oxidized surfaces. Figure 2b shows the PL spectra taken at room temperature of H-terminated ND upon heating in air at gradually elevated temperature (see Experimental Section), here a reverse process, i.e., backward transition from NV° luminescence to NV^- dominated luminescence can be generated upon heating. The first change occurs at about 200 °C. This temperature agrees well with the experimentally observable desorption of adsorbates,[37] confirmed by the loss of the 2DHG surface conductivity (i.e., band bending). At 400 °C permanent changes in the surface termination occur leading to the loss of surface hydrogen due to oxidation, which leads NV^- to dominate the PL spectra.

In addition we observe a large influence of ND size on the PL intensity of both NV° and NV^- defect centers. Figure 2 shows the size effect for hydrogenated ND (Figure 2c) in a biological buffer solution (pH 7, see details in the Supporting Information). ND of various sizes were extracted by centrifugation (see Experimental Section for detail). Both NV^- and NV° centers came from the same irradiation badge and the PL intensity is normalized to the Raman line signal in each ND. For very small particles, even the NV° luminescence can be strongly reduced. For larger particles, the NV^-/NV° ratio is altered by the ND size.

Finally, we demonstrate that the effect of the color shift is observable in a commercial confocal microscope (Figures 2d–g), which opens up a way to use the demonstrated effect for biomolecular sensing in biological environments using commercial methods.

2.3. Investigation of PL from NV Centers Implanted to Different Depths

To verify how the ND compares to high-purity SCD with defined bulk properties, we have used low energy ion implantation (1–6 keV), to produce NV centers to a defined depth and to study its influence on NV color shift changes. Four different sectors in a high-purity SCD were shallow-implanted with nitrogen, using energies 1 keV and 6 keV. Created NV centers were localized from around 3 nm to 10 nm of depth (see Supporting Information). The surface of the SCD was later oxidized and hydrogenated.

To compare the effects observable in our ND particles with undoped high-purity SCD, **Figure 3** shows typical Raman and PL spectra of hydrogenated and oxidized SCD for implantation energies 1 and 6 keV. Though the NV^-/NV° ratio changes clearly with the surface termination, the observed changes are significantly lower than that observed in ND particles. PL emission from NV^- ZPL is also clearly influenced by the implantation energy. For H-terminated SCD on sectors with 6 keV implantation energy (and higher surface conductivity), PL spectra showed decreased emission from NV^- ZPL compared to 1 keV implantation (Figure 3a). To explain the reduction of the effect compared to ND we have performed mathematical modeling.

2.4. Band Bending Model Calculations

The electronic transition (i.e., optical excitation) from NV^- or NV° ground states (^{3}A) to its excited state (^{3}E) occurs by absorbing a photon of energy $h\nu = E_{3E} - E_{3A}$. This is only possible if the NV° or NV^- ground states are originally occupied by a single electron (neutral NV°) or two electrons (negative NV^-). That means E_F must be above the dark ground level of particular NV° or NV^- centers,[7] compared to the 2DHG band bending model in H-terminated undoped diamond[28] in N implanted diamond in which one has to take into account the additional influence of NV^-, NV°, and N defects. These defects will contribute to the total charge balance and influence

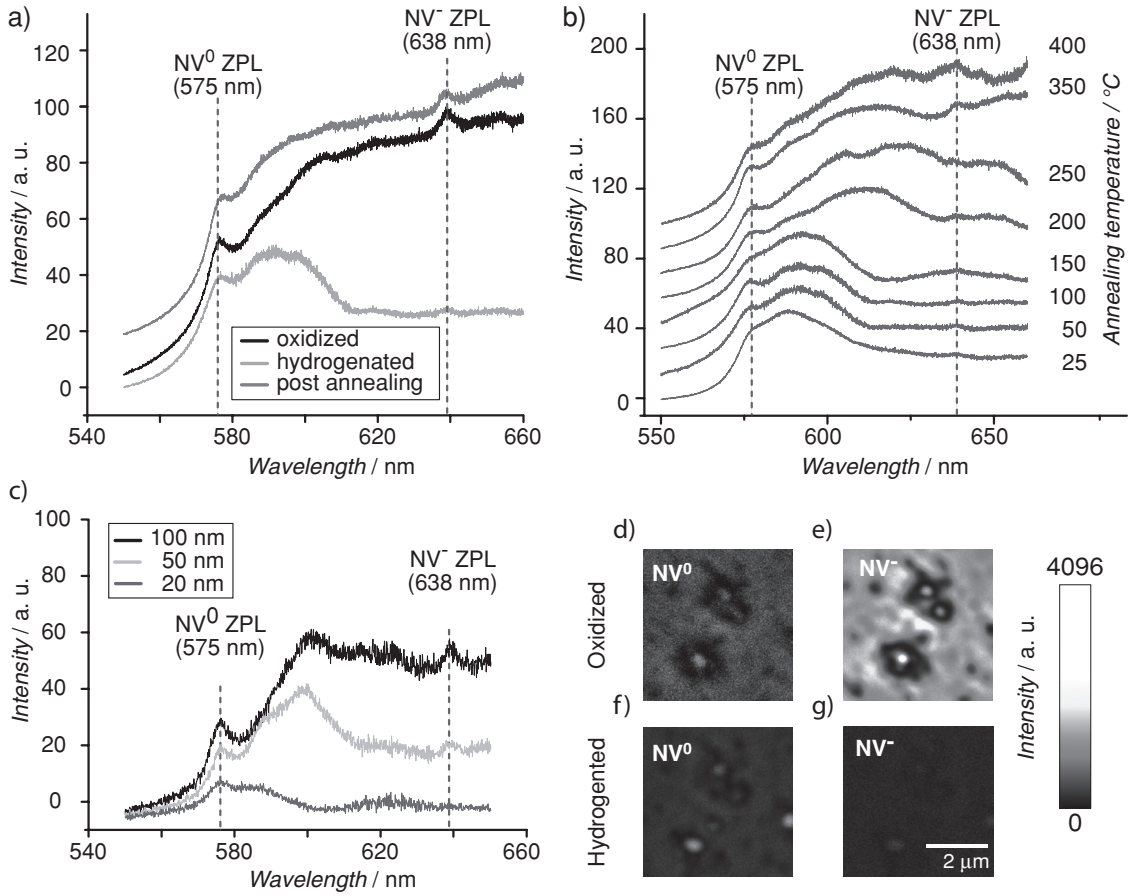

Figure 2. Changes in NV^- and NV° luminescence induced by various terminations of 40 nm sized ND particles. a) Spectra of oxidized, hydrogenated, and annealed surfaces at 400 °C (leading to restoration of original surface termination). The hydrogenation of larger particles (≈40 nm) resulted in luminescence shift towards NV° luminescence (hydrogenated 1). For the smaller particles (<20 nm), the luminescence quenched completely (hydrogenated 2). b) Luminescence changes of hydrogenated ND (40 nm) upon annealing in air at different temperatures. Samples were heated to the target temperature (using a ramp of 25 °C min^{-1}), kept at the set temperature for 30 min and then cooled to room temperature. All spectra were recorded at room temperature and baseline corrected. c) PL spectra of hydrogenated ND of various size (20–100 nm) measured in physiological solution (pH = 7), showing the ND size effect on the PL changes in hydrogenated/oxidized diamond and the possibility to monitor PL changes in liquid, which is essential for biosensor work. The NV^- to NV° ratio could be tuned with the size of ND. All spectra were normalized to the diamond Raman peak and water Raman background was subtracted. d–g) Confocal image of single ND particles upon various treatments. For oxidized ND, both NV° (d) and NV^- (e) luminescence is clearly visible in contrast to hydrogenated ND, where NV° luminescence (f) is dominant and NV^- luminescence (g) is barely visible. Confocal PL images correspond to luminescence collected from 570 nm to 610 nm spectral range for NV° and from 630 nm to 750 nm for NV^-.

the surface band bending (see Figure 1). If the concentration of the donor-like centers (N or NV^-) is increased, the holes from the accumulation layer at an H-terminated surface can be transferred to deep donors by converting N to N^+ and NV^- to NV°. The upwards band bending is then consequently reduced, depending on the concentration of adsorbates.

In our model, the occupation of NV° and NV^- states was calculated from the Boltzmann statistical (concentration of NV centers is in the range of 10^{17} cm^{-3}) distribution, taking into account the presence of N and NV centers at various concentrations. The electric field profile on an H-terminated surface with surface adsorbates is calculated using the Poisson equation for a dielectric medium and energy of $NV^{0/-}$ centers determined from DFT calculations by solving the Schrödinger equation.[24,33] These values for NV° and NV^- energy levels (1.2 eV and 2.0 eV, respectively), are relative to the valence band top. N acts in the model as a deep electron donor with an energy level at 1.7 eV below the conduction band[39] (Figure 1). The detailed model of surface band bending is described in the Supporting Information, which includes an explanation of the equations and constants used.

The results of the numerical simulations for the case of H-termination diamond containing N and NV centers are shown in **Figure 4**. Electrons are transferred from the valence band of diamond to compensate for a charge induced at the diamond surface by adsorbates, which contribute to an upwards surface band bending. The total electric field profile is then the balance between the surface adsorbates and the deep donors (N, NV^-). Our calculation yields a value of ≈2 eV for undoped diamond (i.e., diamond without any NV/N defects), which agrees well with the measured value.[40] However, if additional donors (N, NV^-) are available near the surface, the band bending is reduced.

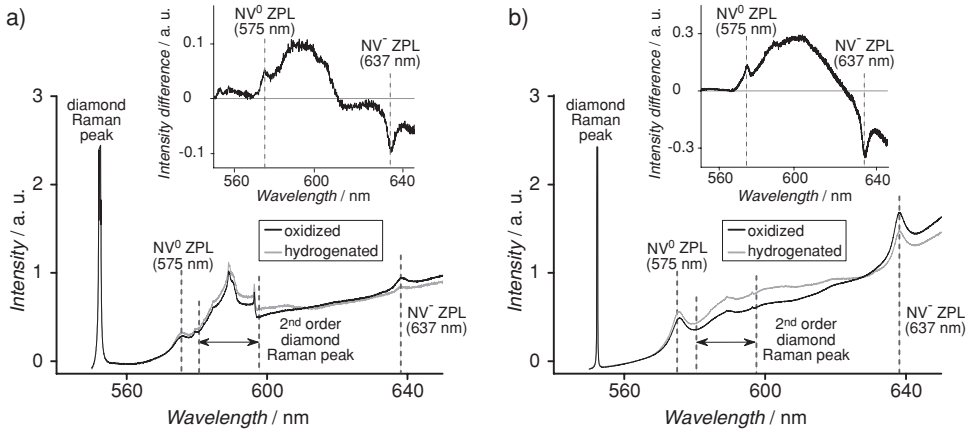

Figure 3. 514-nm-pumped Raman and PL spectra of treated SCD, which show the influence of different surface termination on NV° and NV⁻ related luminescence. NV° ZPL (575 nm) peaks and NV⁻ ZPL (638 nm) peaks are visible for oxidized SCD. For SCD with hydrogenated surface, NV⁻ related luminescence is decreased with an increase in NV° related luminescence, as shown in the difference spectra. All spectra are normalized to the diamond Raman peak (1332 cm^{-1}) and background corrected. a) 1 keV and b) 6 keV N^+ ion implantation energy. When normalized to second order diamond Raman peak, the number of counts (i.e., the intensity) of the NV related luminescence is significantly lower for 1 keV implantation energy compared to 6 keV implantation energy. This fact suggests different efficiency of creation of NV centers depending on the implantation energy for the same total dose, similar as observed in ref. [38]. This effect is discussed below and evaluated in the mathematical modeling of the observed effects.

2.5. Size Effect of ND

Figure 4 compares the band bending calculations,for two model situations, HPHT NDs and implanted SCD. When comparing the modeled data in Figure 4 and the experimental data in Figure 2,3, it is clear that the observed effect of the PL shift is much weaker in SCD then in ND. The influence of H/O termination on PL in the implanted SCD was discussed in previous work[26] and also recently.[25] The enhancement of the PL shift in ND is in agreement with theory for the size-dependent effects in spherical particles outlined above.

There are two reasons for the magnification of the NV°/NV⁻ PL effect in ND compared to SCD. First, N is homogenously distributed in the ND particle and the conversion efficiency from N to NV is higher (vacancy migration during annealing for ND[41]). Additionally, in the case of nanoparticles, the size effect

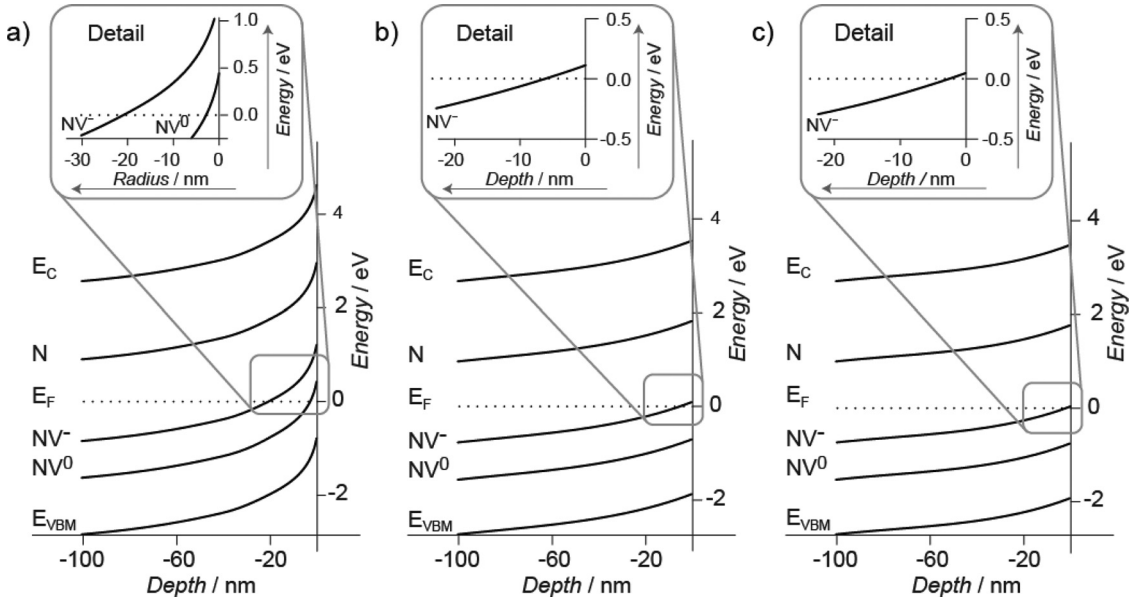

Figure 4. Simulation of electron statistics in hydrogen terminated surfaces using a density of states (DOS) model. Band diagrams show energetic profiles of the conduction band minimum (E_C), valence band maximum (E_{VBM}), NV⁻, NV°, and N impurities relative to the Fermi level (at zero energy) for a) Ib HPHT diamond contained 200 ppm of nitrogen with surface carrier density 10^{13} cm^{-3}, where 10% of nitrogen is converted to NV centers.[41,42] In case of ND particles, we solve the Poisson equation using spherical coordinates. In this case we approximate diamond as an spherical particle. b) IIa diamond plate implanted with nitrogen (6 keV, 10^{13} ions cm^{-2}), surface carrier density 10^{13} cm^{-3} with 1% yield of conversion to NV centers.[38] c) IIa diamond plate implanted with nitrogen (1 keV, 10^{13} ions cm^{-2}), surface carrier density 10^{13} cm^{-3} with 0.1% yield of conversion to NV centers.[38] Cases (b) and (c) are solved using a 1D model as there is no need to calculate 3D effects, which are essential for small nanoparticles.

is important. We consider spherical shaped ND particles and use three dimensions to solve Poisson equations. To describe this situation we have used spherical coordinates (see Figure 4). Taking an example case of a round ND particle (in our case cubo-octahedron) and placing just one NV center in the center of the sphere; i.e., surface density of the charge is proportional to $\frac{4}{3}\pi r^2$, there is direct enhancement of the ratio of the surface charge density to NV concentration compared to SCD, if the particle is sufficiently small (modeling shows that this is up to 40 nm) this leads to the signal enhancement compared to a flat SCD.[25] For NV^- centers, our calculations show that the 3D ND enhancement leads to quenching of NV^- luminescence up to 22 nm of depth in comparison with just a few nanometers for the case of SCD (shown in detail in Figure 4).[25] If the size of the ND particle is sufficiently small a situation can occur where the NV° energy level is actually above the E_F, depending on the concentration of the NV center and nitrogen. This can consequently lead to full quenching of the NV PL. This situation is modeled in detail in the Supporting Information, clearly indicating profound band bending and occupation changes for ND particles compared to SCD.

3. Conclusions

Luminescent properties of NV^- and NV° centers engineered in nanodiamond (ND) particles of 20–100 nm size were studied, aiming at the development of a novel type of ND sensors that are sensitive to the chemical and electrical charge environment. It was found that NV^- luminescence was strongly reduced for the hydrogen-terminated ND surface compared with oxidized diamond. The original NV^-/NV° ratio could be restored by annealing the ND in air at 400 °C. All data (ND and SCD) support our model that the surface band bending can be used to strongly influence the NV^- and NV° luminescence in ND particles. The charge interactions scale as $\approx 1/r^2$, as confirmed by mathematical modeling. The NV^- and NV° luminescence in ND was compared with high-quality, ultrasmooth, IIa diamond, which was shallow implanted by N^+ ions in the surface nanolayer. We clearly saw the PL enhancement in ND. We modeled the enhancement by solving the Poisson equation on 3D coordinates showing that, for ND, PL changes are effective for particles with a size of 40 nm. This effect brings new possibilities for molecular imaging using ND, complementing the FRET technique. We foresee that the observed effects of NV^- PL quenching at the diamond surfaces can serve for optical monitoring of the chemical environment and biomolecular interactions close to the surface of ND particles by chemically induced electrical fields. Recently we have applied the presented effect of NV shifts by attaching charged polymer macromolecules[43] for real-time imaging in liquid in the case of fluorinated and hydrogenated ND. Molecular recognition events in cells are currently being studied by our group.

4. Experimental Section

Materials: Sulfuric acid, nitric acid, hydrochloric acid, and sodium hydroxide were purchased from Penta (Czech Republic) with p. a. purity. High-pressure high-temperature (HPHT)-type Ib ND of 0 to 150 nm size were sourced from Microdiamant AG, Switzerland and contained about 100 ppm nitrogen. SCD CVD type IIa of high purity was purchased from Element 6.

Preparation of Nanodiamond and Diamond Samples: A commercial solution of ND was lyophilized and heated in a slow stream of air at 425 °C for 5 h to remove any sp^2 carbon-containing layer.[44] The resulting pale grey powder was dispersed in water and deposited in the form of a thin film on a target backing (10 mg cm^{-2}) for proton implantation. The ND was then irradiated using an external proton beam of the isochronous cyclotron U-120M. The angle of the target backing with respect to the beam direction was 10°. The fluence of the delivered beam was 9.2×10^{15} cm^{-2}, the beam energy was 5.4 MeV, and the beam current was 0.6 μA. The irradiated ND was thermally annealed in vacuum at 710 °C for 2 h and then oxidized in a mixture of concentrated H_2SO_4-HNO_3 (9:1, v/v)[3] at 90 °C for 7 days. The reaction mixture was diluted with deionized water and the NDs were separated by centrifugation and washed subsequently with 0.1 M NaOH, 0.1 M HCl, and finally three times with water. The solution was lyophilized, providing highly luminescent NDs in the form of a stable colloidal dispersion in water, as confirmed by atomic force microscopy (AFM) and dynamic light scattering (DLS; final size ≈20–100 nm). The colloidal dispersion was stable after 2 months with no sedimentation. A microdroplet of the dispersion was dried on a quartz substrate, producing isolated ND particles, as confirmed by AFM (see Figure S1, Supporting Information). The remainder of the material was lyophilized for later hydrogenation.

A SCD was irradiated with a N^+ ion beam using a low-energy duoplasmatron ion source. The energies of the nitrogen ions were 1 keV and 6 keV with a fluence of 10^{13} cm^{-2}, yielding a total concentration of N in the range of 100s of ppm per exposure, as simulated by TRIM (the stopping and range of ions in matter)[45] (**Figure** 5a). The mean

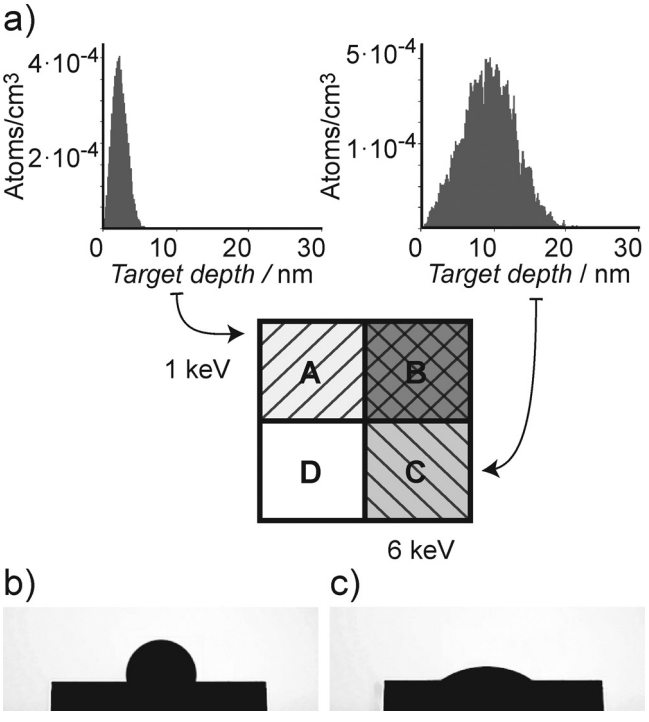

Figure 5. a) Schematic map and TRIM simulation for SCD diamond with four sectors implanted by N^+ ions. Sections A and B were implanted with the same dose 10^{13} cm^{-2}, but different energies (1 and 6 keV, respectively). Sections C and D were implanted twice at the same conditions (dose 10^{13} cm^{-2}, with energies of 1 and 6 keV, respectively). The *y*-axis scale shows implanted atoms in atoms cm^{-3} per 1 carbon atom. Contact angle of b) hydrogenated and c) oxidized SCD.

Table 1. The summary of individual procedures within the experiment.

Experimental Steps	Ib ND Particles	IIa Single Crystal CVD
1) Implantation	protons 5.4 MeV, 9.2×10^{15} atoms cm^{-2}	nitrogen 1 and 6 keV, 6×10^{13} atoms cm^{-2}
2) Annealing	710 °C, 2 h, ultrahigh vacuum (UHV)	700 °C, 2 h,UHV
3) Oxidation	$H_2SO_4 + HNO_3$ (9:1) 90 °C, 7 d	$H_2SO_4 + HNO_3$ (9:1) 90 °C, 7 days
4) Hydrogenation	hydrogen plasma 30 min, 500 °C, 1 mbar	hydrogen plasma 30 min, 500 °C, 1 mbar
5) Oxidation	annealing in air 400 °C, 120 min	$H_2SO_4 + HNO_3$ (9:1) 90 °C, 7 days

projected range in diamond was 3 nm (1 keV) and 10 nm (6 keV). First, implantation was carried out using 1 keV with half of the SCD covered by a mask, after this implantation the crystal was turned by 90° and 6 keV ions were implanted, resulting in four different implantation sectors on one SCD (Figure 5). The implanted SCD was annealed in vacuum at 700 °C for 1 h to create NV centers.[46,47] SCD was then oxidized by exposing it to a mixture of H_2SO_4 and HNO_3 using the same procedure as for the ND.

Surface Treatment: The surface of ND and SCD was cleaned and oxidized after annealing by the methods described above. Hydrogenation of samples was carried out microwave-excited hydrogen plasma for 30 min at a temperature of 500 °C and pressure of 1 mbar, in a vibrating holder using apparatus described previously.[48] Finally, the H-terminated samples (droplets) were annealed for 120 min in air at 400 °C to oxidize the surface. At each step the luminescence spectra were measured at room temperature.

The surface of the SCD after oxidation contained mainly carboxy, carbonyl, hydroxyl, or lactone groups.[49] For the hydrogen-terminated and oxidized SCD the surface contact angles were 92° and 18°, respectively, confirming high efficiency of both hydrogen and oxidation treatments[50] (Figures 5b,c). The individual steps are summarized in **Table 1**.

Luminescence Measurements: The effects of surface termination on the PL of NV centers were studied in two different configurations, using either nanodiamond (ND) particles[51,52] or single crystal diamond (SCD). The luminescence of individual particles was detected by a confocal microscope Olympus FV-1000, with an excitation wavelength of 553 nm and laser power of 15 mW. Raman and luminescence spectra were measured using a Renishaw InVia Raman Microscope, with an excitation wavelength of 514 nm with 25 mW laser power. Spectra were taken at room temperature and normalized to the diamond Raman peak. The AFM measurements were performed in tapping mode (111 kHz) with an NTEGRA Prima NT MDT system equipped with a soft HA_NC etalon tip. The measurements in liquid were performed in a Hellma fluorescence cuvette (type no. 105.252-QS) in aqueous solution (0.2 mg in 1 mL). Size selection was performed by centrifugation. Aqueous colloids were made from particles by immersion of 1 mg of ND into 200 mL of deionized water and dispersing with a high-power ultrasonic horn (Hielscher UP400S, Sonotrode H3) using 400 W at a 1:1 (on/off) cycle for 2 h under liquid cooling. The temperature of the solution was below 25 °C. The solution was centrifuged for 60 min (ref: 14 000 × g). The solution was divided into three fractions with peak distributions around 20 nm, 50 nm, and 100 nm, as confirmed by AFM and DLS. For measurements of luminescence changes upon consecutive annealing of hydrogenated ND in air, samples were heated to the target temperature (using a ramp of 25 °C per min), kept at the set temperature for 30 min, and then cooled to room temperature. At each step the luminescence spectra were measured at room temperature.

Supporting Information

Supporting Information is available from the Wiley Online Library or from the author. It includes a detailed description of the mathematical model of surface band bending, including equations, parameters, and constants used, a figure showing an AFM image of nanodiamonds used in the experiment, and surface conductivity measurements on the SCD, with additional discussion connected to its influence on surface band bending.

Acknowledgements

The authors thank Dr. Jana Poltierova-Vejpravova for annealing the sample and Dr. Ivan Gregora for help with Raman spectroscopy. They also thank Prof. Joerg Wrachtrup, Prof. Fedor Jelezko, and Dr. Friedenman Reinhard from Stuttgart University, as well asJan Richter and Dr. Jan Svoboda for help with the confocal microscopy. The authors acknowledge financial support from the Academy of Sciences of the Czech Republic (grants KAN200100801, KAN301370701, and KAN400480701), the European R&D projects (FP7 ITN Grant No. 238201–MATCON, No. 245122 DINAMO, MATERA_BBM-1955 and COST MP0901–LD 11076 and LD11078), and MSM6840770012 "Transdisciplinary Research in the Field of Biomedical Engineering II".

Received: August 17, 2011
Published online: December 15, 2011

[1] D. Ho, *ACS Nano* **2009**, *3*, 3825.
[2] C. C. Fu, H. Y. Lee, K. Chen, T. S. Lim, H. Y. Wu, P. K. Lin, P. K. Wei, P. H. Tsao, H. C. Chang, W. Fann, *Proc. Natl. Acad. Sci. USA* **2007**, *104*, 727.
[3] Y. R. Chang, H. Y. Lee, K. Chen, C. C. Chang, D. S. Tsai, C. C. Fu, T. S. Lim, Y. K. Tzeng, C. Y. Fang, C. C. Han, H. C. Chang, W. Fann, *Nat. Nanotechnol.* **2008**, *3*, 284.
[4] K. K. Liu, C. L. Cheng, C. C. Chang, J. I. Chao, *Nanotechnology* **2007**, *18*, 325102.
[5] J. Tisler, G. Balasubramanian, B. Naydenov, R. Kolesov, B. Grotz, R. Reuter, J. B. Boudou, P. A. Curmi, M. Sennour, A. Thorel, M. Burscht, K. Aulenbacher, R. Erdmann, P. R. Hemmer, F. Jelezko, J. Wrachtrup, *ACS Nano* **2009**, *3*, 1959.
[6] T. Gaebel, M. Domhan, C. Wittmann, I. Popa, F. Jelezko, J. Rabeau, A. Greentree, S. Prawer, E. Trajkov, P. R. Hemmer, J. Wrachtrup, *Appl. Phys. B* **2006**, *82*, 243.
[7] K. Iakoubovskii, G. J. Adriaenssens, M. Nesladek, *J. Phys.: Cond. Matter* **2000**, *12*, 189.
[8] S. J. Yu, M. W. Kang, H. C. Chang, K. M. Chen, Y. C. Yu, *J. Am. Chem. Soc.* **2005**, *127*, 17604.
[9] Y. Yuan, Y. Chen, Y. H. Liu, H. Wang, Y. Liu, *Diamond Relat. Mater.* **2009**, *18*, 95
[10] Y. Liang, M. Ozawa, A. Krueger, *ACS Nano* **2009**, *3*, 2288.
[11] X. Q. Zhang, M. Chen, R. Lam, X. Xu, E. Osawa, D. Ho, *ACS Nano* **2009**, *3*, 2609.
[12] O. Faklaris, V. Joshi, T. Irinopoulou, P. Tauc, M. Sennour, H. Girard, C. Gesset, J. C. Arnault, A. Thorel, J. B. Boudou, P. A. Curmi, F. Treussart, *ACS Nano* **2009**, *3*, 3955.
[13] H. Huang, E. Pierstorff, E. Osawa, D. Ho, *ACS Nano* **2008**, *2*, 203.
[14] R. Martn, M. lvaro, J. R. Herance, H. Garca, *ACS Nano* **2010**, *4*, 65.

[15] M. Chen, E. D. Pierstorff, R. Lam, S. Y. Li, H. Huang, E. Osawa, D. Ho, *ACS Nano* **2009**, *3*, 2016.
[16] K. K. Liu, W. W. Zheng, C. C. Wang, Y. C. Chiu, C. L. Cheng, Y. S. Lo, C. Chen, J. I. Chao, *Nanotechnology* **2010**, *21*, 315106.
[17] C. Bradac, T. Gaebel, N. Naidoo, M. J. Sellars, J. Twamley, L. J. Brown, A. S. Barnard, T. Plakhotnik, A. V. Zvyagin, J. R. Rabeau, *Nat. Nanotechnol.* **2010**, *5*, 345.
[18] F. Maier, M. Riedel, B. Mantel, J. Ristein, L. Ley, *Phys. Rev. Lett.* **2000**, *16*, 3472.
[19] P. Strobel, M. Riedel, J. Ristein, L. Ley, *Nature* **2004**, *430*, 439.
[20] C. E. Nebel, C. Sauerer, F. Ertl, M. Stutzmann, C. F. O. Graeff, P. Bergonzo, O. A. Williams, R. Jackman, *Appl. Phys. Lett.* **2001**, *79*, 4541.
[21] G. Davies, M. F. Hamer, *Proc. R. Soc. Lond. A* **1976**, *348*, 285.
[22] S. C. Lawson, D. Fisher, D. C. Hunt, M. E. Newton, *J. Phys.: Condens. Matter* **1998**, *10*, 6171.
[23] N. Mohan, Y. K. Tzeng, L. Yang, Y. Y. Chen, Y. Y Hui, C. Y. Fang, H. C. Chang, *Adv. Mater.* **2010**, *22*, 843.
[24] J. P. Goss, P. R. Briddon, R. Jones, S. Sque, M. J. Rayson, *Phys. Rev. B* **2005**, *72*, 035214.
[25] M. V. Hauf, B. Grotz, B. Naydenov, M. Dankerl, S. Pezzagna, J. Meijer, F. Jelezko, J. Wrachtrup, M. Stutzmann, F. Reinhard, J. A. Garrido, *Phys. Rev. B* **2011**, *8*, 83.
[26] M. Nesladek, V. Rezacova, A. Kovalenko, I. Kratochvilova, V. Kocka, EMRS Spring Meeting, Strasbourg, June 2010, http://www.emrs-strasbourg.com/files/USB%2010/symposium_d.pdf (December 2011).
[27] J. Ristein, M. Riedel, L. Ley, *J. Electrochem. Soc.* **2004**, *151*, 315.
[28] C. E. Nebel, *New Diamond Front. Carbon Technol.* **2005**, *15*, 247.
[29] B. Rezek, D. Shin, H. Watanabe, C. E. Nebel, *Sens. Actuators B* **2007**, *122*, 596.
[30] J. A. Garrido, A. Hardl, S. Kuch, M. Stutzmann, O. A. Williams, R. B Jackmann, *Appl. Phys. Lett.* **2005**, *86*, 073504.
[31] A. Hartl, E. Schmich, J. A. Garrido, J. Hernando, C. R. Catharino, S. Walter, P. Feulner, A. Kromka, D. Steinmuller, M. Stutzmann, *Nat. Mater.* **2004**, *3*, 736.
[32] B. Rezek, M. Kratka, A. Kromka, M. Kalbacova, *Biosens. Bioelectron.* **2010**, *26*, 1307.
[33] J. P. Goss, P. R. Briddon, R. Jones, S. Sque, *Diamond Relat. Mater.* **2004**, *13*, 351.
[34] I. Kratochvilova, A. Taylor, A. Kovalenko, F. Fendrych, V. Rezacova, V. Petrak, S. Zalis, J. Sebera, M. Nesladek, *Mater. Res. Soc. Symp. Proc.* **2010**, *1203*, J03.
[35] K. M. C. Fu, C. Santori, P. E. Barclay, R. G. Beausoleil, *Appl. Phys. Lett.* **2010**, *96*, 121907
[36] O. A. Williams, J. Hees, C. Dieker, W. Jger, L. Kirste, C. E. Nebel, *ACS Nano* **2010**, *4*, 4824.
[37] M. Nesladek, L. M. Stals, A. Stesmans, K. Iakoubovskij, G. J. Adriaenssens, *Appl. Phys. Lett.* **1998**, *72*, 3306.
[38] S. Pazzagna, B. Naydenov, F. Jelezko, J. Wratchup, J. Meijer, *New J. Phys.* **2010**, *12*, 065017.
[39] J. Ristein, M. Riedel, M. Stammler, B. F. Mantel, L. Ley, *Diamond Relat. Mater.* **2002**, *11*, 359.
[40] B. Rezek, C. Sauerer, C. E. Nebel, M. Stutzmann, J. Ristein, L. Ley, E. Snidero, P. Bergonzo, *Appl. Phys. Lett.* **2003**, *82*, 14.
[41] J. P. Boudou, P. A. Curmi, F. Jelezko, J. Wrachtrup, P. Aubert, M. Sennour, G. Balasubramanian, R. Reuter, A. Thorel, E. Gaffet, *Nanotechnology* **2009**, *20*, 5602.
[42] C. Santori, P. E. Barclay, K. C. Fu, R. G. Beausoleil, *Phys. Rev. B* **2009**, *79*, 5313.
[43] V. Rezacova, M. Nesladek, P. Cigler, M. Ledvina, J. Kucka, J. Stursa, J. Ralis, J. Vacik, P. Mojzes, A. Taylor, I. Kratochvilova, F. Fendrych, MRS Fall Meeting, Boston, Nov. 2010, Abstract No. A7.5, http://www.mrs.org/s_mrs/doc.asp?CID = 27791&DID = 332936 (August 2011).
[44] S. Osswald, G. Yushin, V. Mochalin, S. O. Kucheyev, Y. Gogotsi, *J. Am. Chem. Soc.* **2006**, *128*, 11635.
[45] J. Zeigler, SRIM- **2008**, http://srim.org (December 2011).
[46] L. Allers, A. T. Collins, J. Hiscock, *Diamond Relat. Mater.* **1998**, *7*, 228.
[47] K. Iakoubovskii, G. J. Adriaenssens, *J. Phys.: Condens. Matter* **2001**, *13*, 6015.
[48] A. Taylor, F. Fendrych, L. Fekete, J. Vlček, V. Řezáčová, V. Petrák, J. Krucký, M. Nesládek, M. Liehr, *Diamond Relat. Mater.* **2011**, *20*, 613.
[49] P. Cigler, M. Ledvina, M. Tvrdonova, V. Rezacova, M. Nesladek, I. Kratochvilova, F. Fendrych, J. Stursa, J. Kucka, J. Ralis, Abstr. 2nd International Conference, Conference proceedings, Nanocon 2010 Olomouc, Czech Republic, October 12–14, 2010.
[50] L. Ostrovskaya, V. Perevertailo, V. Ralchenko, A. Dementjev, O. Loginova, *Diamond Relat. Mater.* **2002**, *11*, 845.
[51] A. M. Schrand, S. A. C. Hens, O. A. Shenderova, *Crit. Rev. Solid State Mater. Sci.* **2009**, *34*, 18.
[52] A. Kreuger, *J. Mater. Chem.* **2008**, *18*, 1485.